UC Irvine
UC Irvine Previously Published Works

Title

Spatial Transcriptomics reveals a T cell-mediated microglial activation axis of neurodegeneration following immune checkpoint inhibition

Permalink

https://escholarship.org/uc/item/58z1c9hs

Authors

Swami, Devyani
Sureshchandra, Suhas
Vinnakota, Janaki Manoja
et al.

Publication Date

2026-06-11

DOI

10.64898/2026.06.10.730982

Copyright Information

This work is made available under the terms of a Creative Commons Attribution License, available at https://creativecommons.org/licenses/by/4.0/

eScholarship.org Powered by the California Digital Library
University of California

Targeting Complement Signaling to Limit Immune Checkpoint Inhibition-related Neuroinflammation

Kelly M. Nguyen[1], An H. Do[1], Devyani Swami[1], Tracy Nguyen[1], Mihika G. Jalwadi[1], Andrea J. Tenner[2], Shivashankar Othy[1], Munjal M. Acharya[1*]

[1]School of Medicine, University of California, Irvine, Irvine, United States, [2]University of California Irvine, Irvine, United States

Submitted to Journal:
Frontiers in Immunology

Specialty Section:
Cancer Immunity and Immunotherapy

Article type:
Brief Research Report Article

Manuscript ID:
1998741

Received on:
15 Sep 2026

Revised on:
29 Oct 2026

Journal website link:
www.frontiersin.org

In review

Scope Statement

This manuscript directly aligns with the Research Topic's focus on microglial biology, CNS immune mechanisms, and translational immunotherapeutic strategies. We demonstrate that immune checkpoint inhibition (ICI) in melanoma elevates microglial C5aR1 expression, both in postmortem human brain tissue and mouse models, identifying complement signaling as a critical mediator linking systemic cancer immunotherapy to CNS neuroinflammation. Our findings elucidate a molecular mechanism governing microglial activation and astrogliosis, directly addressing the Topic's emphasis on understanding how microglial dysfunction contributes to disease initiation and progression. Furthermore, genetic targeting of C5aR1 not only attenuates neuroinflammation but also suppresses tumor growth without compromising ICI's anti-tumor efficacy, exemplifying the Topic's goal of developing brain-targeted immunotherapies that engage microglia therapeutically. By bridging mechanistic insight into complement-driven microglial activation with a clinically relevant strategy to mitigate immune-related adverse events (irAEs), this work advances the field of CNS immune regulation and neuro-oncology. These contributions are well-suited to this collection's mission of charting a path from foundational microglial biology to next-generation precision immunotherapies that preserve neurological function and extend brain health span.

Conflict of interest statement

The authors declare a potential conflict of interest and state it below

The author(s) declared that they were not an editorial board member of Frontiers, at the time of submission.

In review

Credit Author Statement

An H Do: Data curation, Formal Analysis, Investigation, Methodology, Writing – original draft. **Andrea Joan Tenner**: Visualization, Writing – original draft, Writing – review & editing. **Kelly MC Nguyen**: Data curation, Formal Analysis, Investigation, Methodology, Visualization, Writing – original draft, Writing – review & editing. **Munjal M Acharya**: Conceptualization, Data curation, Funding acquisition, Project administration, Resources, Supervision, Writing – original draft, Writing – review & editing. **Mihika G Jalwadi**: Investigation, Methodology, Writing – original draft. **Shivashankar Othy**: Funding acquisition, Resources, Supervision, Visualization, Writing – original draft, Writing – review & editing. **Devyani Swami**: Data curation, Formal Analysis, Investigation, Methodology, Validation, Visualization, Writing – original draft. **Tracy Nguyen**: Data curation, Investigation, Methodology, Writing – original draft.

Keywords

anaphylatoxin, anti-CTLA-4, anti-PD-1, Astrocytes, C5a, C5aR1, complement cascade, immune checkpoint inhibition

Abstract

Word count: 180

Immune checkpoint inhibition (ICI) has transformed cancer therapy by targeting inhibitory constraints on T cells, thereby enhancing antitumor immunity. However, emerging evidence indicates that ICI can also provoke neuroinflammatory responses leading to adverse neurological outcomes. Complement anaphylatoxin signaling, especially the C5a-C5aR1 axis, has been implicated in driving cancer therapy-associated neuroinflammation, and its inhibition has shown neuroprotective effects in mouse models of cranial irradiation and neurodegenerative diseases. Here, we report elevated microglial C5aR1 expression in the postmortem brains from ICI-treated patients. Based on this, we investigated the impact of genetic targeting of C5aR1 (C5aR1-KO) in melanoma-bearing mice treated with ICI by assessing tumor progression along with neuroinflammation, including microglial activation and astrogliosis. C5aR1 deficiency suppresses tumor growth over time without compromising the antitumor function of ICI. Importantly, C5aR1-KO significantly attenuated microglial activation and astrogliosis post-ICI treatment. These results identify complement signaling as a critical mediator that links systemic immunotherapy to neuroinflammation. Thus, targeting the C5a-C5aR1 pathway is a promising strategy to mitigate immune-related adverse events (irAEs), preserve neurological function, and spare anti-tumor immunity, ultimately improving quality of life in melanoma survivors.

Funding information

This work was supported by the National Institutes of Health (NIH) awards (R01CA251110, R01CA262213) to M.M.A., NIH NIAID R01AI121945 and R21AI144823 to S.O., Defense Health Agency award (ME250313) to S. O. and M. M. A. UCI CFCCC GRTH was supported by the NIH program project award P30CA062203.

Funding statement

The author(s) declare that financial support was received for the research and/or publication of this article.

Ethics statements

Studies involving animal subjects

Generated Statement: The animal study was approved by University of Irvine Institutional Animal Care & Use Committee. The study was conducted in accordance with the local legislation and institutional requirements.

Studies involving human subjects

Generated Statement: The studies involving humans were approved by University of Freiburg Ethics Committee (protocol number 340/19). The studies were conducted in accordance with the local legislation and institutional requirements. The participants provided their written informed consent to participate in this study.

Inclusion of identifiable human data

Generated Statement: No potentially identifiable images or data are presented in this study.

Data availability statement

Generated Statement: The original contributions presented in the study are included in the article/supplementary material, further inquiries can be directed to the corresponding author/s.

Generative AI disclosure

No Generative AI was used in the preparation of this manuscript.

In review

Brief Research Report (short communication)

Targeting Complement Signaling to Limit Immune Checkpoint Inhibition-related Neuroinflammation

Kelly M. C. Nguyen[1], An H. Do[1], Devyani Swami[1], Tracy N. Nguyen[1], Mihika G. Jalwadi[1], Andrea J. Tenner[2], Shivashankar Othy[3], Munjal M. Acharya[1,4,*]

[1]Department of Anatomy & Neurobiology, [2]Department of Molecular Biology & Biochemistry,[3]Department of Physiology & Biophysics, [4]Department of Radiation Oncology, School of Medicine, University of California, Irvine

In review

***Corresponding author:**

Dr. Munjal M. Acharya
Associate Professor
Department of Anatomy & Neurobiology
Department of Radiation Oncology (Joint)
School of Medicine, University of California, Irvine
Email: macharya@uci.edu
ORCID: 0000-0002-7767-5642

Running title: C5aR1-KO protects against ICI-induced neuroinflammation

Keywords: Immune checkpoint inhibition, anti-PD-1, anti-CTLA-4, complement cascade, anaphylatoxin, C5a, C5aR1, microglia activation, astrocytes, neuroinflammation

ABSTRACT

Immune checkpoint inhibition (ICI) has transformed cancer therapy by targeting inhibitory constraints on T cells, thereby enhancing antitumor immunity. However, emerging evidence indicates that ICI can also provoke neuroinflammatory responses leading to adverse neurological outcomes. Complement anaphylatoxin signaling, especially the C5a-C5aR1 axis, has been implicated in driving cancer therapy-associated neuroinflammation, and its inhibition has shown neuroprotective effects in mouse models of cranial irradiation and neurodegenerative diseases. Here, we report elevated microglial C5aR1 expression in the postmortem brains from ICI-treated patients. Based on this, we investigated the impact of genetic targeting of C5aR1 (C5aR1-KO) in melanoma-bearing mice treated with ICI by assessing tumor progression along with neuroinflammation, including microglial activation and astrogliosis. C5aR1 deficiency suppresses tumor growth over time without compromising the antitumor function of ICI. Importantly, C5aR1-KO significantly attenuated microglial activation and astrogliosis post-ICI treatment. These results identify complement signaling as a critical mediator that links systemic immunotherapy to neuroinflammation. Thus, targeting the C5a-C5aR1 pathway is a promising strategy to mitigate immune-related adverse events (irAEs), preserve neurological function, and spare anti-tumor immunity, ultimately improving quality of life in melanoma survivors.

In review

1 | INTRODUCTION

Immune checkpoint inhibitor (ICI) therapies are highly effective treatments across multiple cancer types, with particularly significant improvements in therapeutic outcomes for melanoma (1-3). ICIs, including antibodies targeting cytotoxic T lymphocyte antigen-4 (CTLA-4) and programmed cell death protein 1 (PD-1), enhance antitumor immunity by blocking inhibitory signaling pathways that restrain T cell activation (1, 2, 4). However, accumulating evidence indicates that ICI treatment can also induce immune-related adverse events (irAEs), including neurodegenerative sequelae (5-7). These effects are characterized by elevated neuroinflammation, including increased infiltration and activation of T cells, expansion of MHC-II$^+$ myeloid populations, and pronounced microglial activation, and interaction of activated T cells and microglia, ultimately contributing to degradation of synaptic and myelin integrity and neurocognitive decline (8-10). Clinically, cancer survivors have reported neurocognitive impairments following ICI therapy, underscoring a significant unmet need to mitigate CNS toxicity and improve quality of life in melanoma survivors (7, 11-13) .

A major driver of neuroinflammation associated with other cancer therapies is elevated pro-inflammatory mediators, including components of the CNS complement cascade (14). Using both genetic and pharmacological approaches, our prior work has demonstrated that complement proteins and receptors, particularly C1q and C5aR1, play key roles in mediating neuroinflammation and neurodegeneration following cranial radiation therapy (RT) for brain cancer, contributing to cognitive impairment (15, 16). The complement cleavage product C5a, an anaphylatoxin, promotes robust pro-inflammatory polarization of microglia through engagement of its receptor C5aR1, as observed in Alzheimer's disease (AD) and RT-exposed brains (14, 15, 17). Accordingly, ablation of the C5a-C5aR1 axis via genetic knockout of C5aR1 or pharmacological targeting of C5aR1 signaling protected against microglial activation and improved cognitive outcomes in both AD and cranial irradiation models (14, 15, 17).

Anti-PD-1 treatment has been shown to elevate proinflammatory serum complement cascade components, including C3a, C5a, Factors H and I, which were associated with ICI-induced adverse consequences (18, 19). Building on these findings, this study investigates the role of microglial complement signaling in ICI-associated neuroinflammation and evaluates the potential of targeting complement anaphylatoxin receptor 1 (C5aR1) as a neuroprotective strategy. We first confirmed C5aR1 expression in postmortem brains from ICI-treated patients. Then, using a syngeneic murine melanoma model in WT and C5aR1-KO mice, we evaluated the impact of melanoma burden and combination ICI therapy (anti-PD-1 and anti-CTLA-4) on tumor progression and CNS gliosis, with a particular focus on microglial activation.

In review

2 | METHODS

2.1 Animals and Treatments

All animal experimentation procedures are in accordance with the guidelines provided by NIH and approved by the University of California, Irvine (UCI) Institutional Animal Care and Use Committee (IACUC). Two mouse lines (12-13 weeks of age) were used: male wildtype (WT, C57BL/6J, Jackson Laboratory) and C5aR1-KO (kind gift from R. A. Wetsel)(20). WT and C5aR1-KO mice were divided into the following groups (N = 8-10 mice per group): *i)* vehicle (PBS) treated, *ii)* melanoma-bearing mice receiving vehicle (induced using murine D4M-3A.UV2 line) as described (8), *iii)* combination ICI-treated (anti-PD1, 200 µg, 3 times weekly, and anti-CTLA-4, 1000 µg, 2 times weekly, i.p.), and *iv)* melanoma-bearing mice treated with ICI regimen for 3 weeks. We selected this combination ICI regimen based on our previous studies, which showed antitumor responses in melanoma concurrently with neurocognitive decline, gliosis, synaptic loss, and cellular and transcriptomic neuroimmune dysregulation (8, 10). A syngeneic orthotopic model of murine melanoma was developed following bilateral intradermal injections of 5×10^5 D4M-3A.UV2 cells were injected into the underbelly tent in WT or C5aR1-KO mice (Research Design, **Fig. 1E**). D4M-3A.UV2 mouse melanoma cells were cultured in Dulbecco's Modified Eagle Medium/Nutrient Mixture F-12 (1× DMEM/F-12, Gibco) supplemented with 10% HyClone Characterized FBS (fetal bovine serum, Cytiva). Vehicle (PBS) or ICI treatments were initiated one week post-tumor implantation. These murine D4M-3A.UV2 tumors do not metastasize to the brain as shown previously (8). Tumors were measured twice a week for 1 month using a digital caliper to monitor growth and mouse health. The maximum (MD) and perpendicular (PD) tumor diameters were measured for each tumors and the tumor volume (mm^3) was calculated by the following formula:

$$V_t = 0.5 \times MD \times PD^2$$

Tumor-bearing, vehicle-treated WT and C5aR1-KO mice were euthanized one month post-tumor induction, considering humane endpoints. ICI-treated WT and C5aR1-KO cohorts were euthanized one month post-ICI treatment via intracardiac perfusion using 1× PBS-heparin (10 U/ml) followed by ice-cold 4% paraformaldehyde made in PBS (Sigma-Aldrich). Brains were cryoprotected (10-30% sucrose gradient) and sectioned coronally into 30 µm sections as described (16).

2.2. Immunofluorescence staining

2.2.1. Human brains. Formalin-fixed post-mortem human frontal cortex sections (3 µm thick) from three ICI-treated or three age-matched, non-tumor control brains were kind gifts from

In review

the Department of Nuclear Medicine, Medical Center, University of Freiburg, with appropriate patient consent for the donation, storage, and use of the biological materials and collection, and approved by the ethics committee (protocol number 340/19, Analysis of CNS autopsy material and CSF in patients that received anti-PD-1 immunotherapy, Dr. Robert Zeiser), as described (9). UC Irvine Institutional Biosafety Committee (IBC) approved the use of human brain sections for this study (protocol number BUA-R218). Details about patient age, tumor type, health condition, etc. are provided in **Table 1**. ICI-treated patients were male, with a median age of 65 years, and were treated with anti-PD-1, including pembrolizumab, nivolumab, or combined ipilimumab and nivolumab, for the treatment of lung cancer, melanoma, and head and neck cancer. The non-cancer and no therapy control group included two males and one female. Three tissue sections per case were stained for microglia (IBA1) and C5aR1 dual-immunofluorescence staining to capture 3-4 non-overlapping regions of interest (ROI) using laser scanning confocal microscopy and 3D algorithm-based volumetric quantification of co-labeling. Primary antibodies include rabbit anti-IBA-1 (1:500, FUJIFILM Wako, Cat# 019-19741), anti-human C5aR1 antibody (1:350, purified Mouse IgG2a, κ isotype, Biolegend, Cat# 344302). Secondary antibodies include goat anti-rabbit Alexa Fluor 488 (1:500, FisherSci, Cat# a11008; RRID: AB_143165), and goat anti-mouse Alexa Fluor 647 (1:500, Abcam, Cat# ab150115; RRID: AB_2687948). For the dual-immunofluorescence staining, slides containing human cortices were deparaffinized using Histo-Clear (20 min), and dehydrated in 100%, 90%, and 70% ethanol for 3 min each, followed by a distilled water rinse (1 min). Antigen retrieval was facilitated by citrate buffer incubation (10 mM, pH 6.0, microwave treatment for 3-4 min), distilled water washing (1 min), and equilibration using 1× TBST buffer (Tris buffer saline with Tween-20)twice for 5 mins). Sections were then blocked in a humidified chamber using 10% normal goat serum (NGS) containing 5% BSA in 1× TBST for 90 min at room temperature. After that, sections were treated with a mixture of primary antibodies in 1% BSA, 1% NGS in 1× TBST) and incubated overnight at 4 °C. Before secondary antibody treatment, slides were washed in 1× TBST (3 times for 5 min each) and then incubated with the appropriate secondary antibodies using the same incubation buffer as primary antibodies for 60 min at room temperature. After distilled water and 1× TBST rinses, slides were stained with DAPI made in PBS for 10 min (1 µmol/L, FisherSci, Cat# D1306, RRID:AB_2629482) for nuclear staining, followed by a final wash in 1× TBST (10 min) and mounting using (Vectashield, Vector Labs, Cat# H-1000-10).

In review

Group	ICI Therapy	Control
No. of Patients	3	3
Gender (N)	Female (0)	Female (1)
	Male (3)	Male (2)
Age, Median	65 (59-73)	59 (26-70)
Therapy regime	Pembrolizumab (1)	Nil
	Nivolumab(1)	
	Ipilimumab/Nivolumab (1)	

Table 1. Human patient characteristics for the brain biopsy samples used for immunofluorescence analysis.

2.2.2. Mouse brains. For CD68-IBA1 dual immunostaining, mouse brain tissues containing hippocampal sections were washed with 1× PBS-0.3% Tween 20, then incubated in 1× PBS-3% hydrogen peroxide and 1% methanol, followed by a 1× PBS wash and blocking in 1× PBS with 4% BSA and 0.3% Tween 20. Following blocking, sections were immune-stained for CD68 (1:500, rat anti-mouse CD68, Bio-Rad) and IBA-1 (1:500 rabbit anti-IBA-1, FUJIFILM Wako) in 1× PBS containing 1% BSA and 0.3% Tween-20 buffer. Twenty-four hours later, the tissues were washed and stained with secondary antibodies using goat anti-rat Alexa Fluor 647 (1:1000, Abcam) and goat anti-rabbit Alexa Fluor 488 1:500, (FisherSci) for CD68 and IBA-1, respectively.

For TLR4-GFAP, mouse hippocampal brain tissues were washed three times in 1× PBS before blocking in 10% BSA and PBS-0.1% Triton X-100 for 75 minutes at room temperature. This was followed by a primary antibody incubation against TLR4 (1:200, mouse anti-TLR4, Novus) and GFAP (1:500, rabbit anti-GFAP, Bio Legend) in 10% NGS and PBS containing 0.01% Triton X-100 at 4 °C for 48 hours. Afterward, tissue sections were washed three times with 1× PBS, and fluorescent color development was facilitated with secondary antibodies: goat anti-mouse Alexa Fluor 568 (1:200) and goat anti-rabbit Alexa Fluor 488 (1:500) in 10% NGS and PBS containing 0.01% Triton X-100. For all immunostaining, mouse tissues were washed, counterstained with DAPI, and mounted on Superfrost slides using VectaShield antifade mounting medium.

2.3. Microscopy and 3D Algorithm-based Volumetric Quantification. Immunostained brain sections were scanned at high resolution using a laser-scanning confocal microscope (Nikon Eclipse Ti2 AX, Japan) equipped with a 20× PlanApo lens or 40× oil-immersion Plan Fluor lens and a NIS-Elements AR interface. A laser-scanning confocal microscope (Nikon Eclipse Ti2 AX) was used to image the immuno-stained brain sections through 24-25 µm mouse brain sections (0.5 µm thickness per z stack) at voxel size 0.428 × 0.428 × 0.500 and in 2048, 2048 and 29 xyz resolution and 3 µm for human brain tissues (0.158 µm thickness per z stack) at a voxel size of 0.431 × 0.431 × 0.120 µm and at 1024 × 1024 × 27 xyz to obtain 19-20 optical slices and to render

In review

high resolution images for the volumetric quantification of immunoreactivity. Acquisition of confocal z stacks and 3D algorithm-based unbiased volumetric quantification of immunofluorescence (refractive Index 1.5, distance 6.60 µm, gamma correction 0.950, and baseline subtraction 150 AU) were carried out as described in detail previously (15, 16). Each mouse brain section was imaged using 20-24 z stacks, 0.5 µm thick, from the hippocampal dentate gyrus (DG) or dentate hilus (DH) at voxel size 0.428 × 0.428 × 0.500 and in 2048, 2048 and 29 xyz resolution and 3 µm for human brain tissues (z stack thickness 0.158 µm) at a voxel size of 0.431 × 0.431 × 0.120 µm and at 1024 × 1024 × 27 xyz to obtain 19-20 optical slices and to create surface or puncta rendering of high resolution images for the volumetric quantification of immunoreactivity. 3D surface renderings of the volume (immunofluorescence) were created for each marker using Imaris (v10.1.0, Oxford Instruments), and each channel was analyzed separately. A set of image-processing parameters (e.g., deconvolution, baseline subtraction) was applied to each z stack across all experimental groups, as described previously (15, 16). To determine the co-localization volume between the 3D reconstructed surfaces of two markers for each immunostain, Imaris (v10.1) was used for statistical analysis. This was carried out by directly quantifying the number of voxels from one marker's surface that intersect or occupy the same 3D space as another marker's surface (i.e., the volume of overlap). We did not create a separate colocalization channel. The volume of each colocalized immunoreactive surface of interest was normalized to the control, and the data were expressed as a mean percent immunoreactivity relative to controls.

In review

2.4. Statistical Analysis

Statistical analyses were carried out using GraphPad Prism (v10). An unpaired two-tailed *t* test was performed to compare IBA1/C5aR1 expression in human and mouse brains in control and ICI cohorts. Two-way ANOVA followed by Bonferroni's multiple comparisons test was performed for cancer growth analysis. For all immunohistochemical analyses, three-way ANOVA was performed. Eight experimental groups were included: WT and C5ar1-KO mice under four conditions: vehicle, melanoma, ICI treatment, and melanoma + ICI. Three independent factors were evaluated: genotype (WT vs. C5aR1-KO), melanoma status, and ICI treatment. Three independent factors were evaluated: genotype (WT vs. KO), melanoma status (with vs. without), and ICI treatment (vehicle vs. ICI). The main effects of each factor, along with their two-way interactions (genotype × melanoma, genotype × ICI, and melanoma × ICI) and three-way interaction (genotype × melanoma × ICI), were assessed to determine their influence on CD68/IBA1 and GFAP/TLR4 colocalization. Bonferroni's multiple-comparisons test was

performed for post hoc pairwise comparisons between experimental groups. All results are expressed as mean ± SEM. A p-value of ≤ 0.05 was considered statistically significant.

3 | RESULTS

3.1. Elevated microglial C5aR1 expression in the ICI-treated patient brains

To assess C5aR1 expression in human brains exposed to ICI, we performed dual immunofluorescence staining for a pan-microglial marker (IBA1) and C5aR1 in frontal cortex from postmortem human brain tissue. We compared non-cancer, no-therapy control subject brains with patients treated with ICI (anti-PD-1) for different malignancies. Untreated human brain tissue from cancer-bearing individuals was unavailable. 3D algorithm-based volumetric quantification (Imaris) of IBA1-C5aR1 co-localization was conducted as described previously (15, 16). Anti-PD-1-treated patients (ICI patients') showed significantly increased IBA1-C5aR1 co-labeling (**Fig. 1A**) and immunoreactivity volumes (**Fig. 1B**) compared with non-cancer control patient brains ($p<0.0001$). We found a similar elevation in microglial C5aR1 expression following combination ICI treatment as in the non-cancer mouse hippocampus 8 weeks post-treatment compared to the vehicle-treated controls ($p<0.02$, **Fig. 1C-D**). The relevant Manders coefficients (Mean ± SEM) for human tissues were 0.334 ± 0.081 (N = 3) and 0.576 ± 0.105 (N = 3) for the Control and ICI patients, respectively. In mouse tissues, the coefficients were 0.822 ± 0.041 (N = 5) and 0.812 ± 0.053 (N = 5) in the Control and WT-ICI groups, respectively. These data indicate elevated microglial C5aR1 expression in ICI-treated cancer patients and provide a rationale for a mechanistic murine study.

3.2. C5aR1 KO reduces tumor progression independent of ICI treatment

Disruption of the C5a-C5aR1 signaling axis has been shown to reduce primary and metastatic tumor growth in multiple cancers (1, 2). However, this efficacy in the presence of ICI remains to be studied. To investigate how C5aR1-KO affects melanoma cell proliferation with and without ICI therapy, we plotted the average volume of bilateral tumor sites per mouse over 28 days (Fig. 1C). By Day 28, the WT-MEL group showed the most progressive tumor growth compared with all groups (**Fig. 1F-G**). Conversely, C5aR1-KO mice (C5aR1-KO-MEL group) showed significantly slower tumor growth and smaller tumors than their WT counterparts at the same time point ($p<0.05$ for Day 26, $p<0.0001$ for Day 28). As expected, ICI treatment significantly reduced tumor growth in WT and C5aR1-KO mice, and tumors were not detectable by Day 28 ($p<0.0001$ for WT; $p<0.01$ for C5aR1-KO). In summary, C5aR1-KO reduced tumor progression, ICI treatment

In review

effectively countered melanoma growth over time, and, importantly, C5aR1-KO background did not interfere with ICI therapeutic efficacy (**Fig. 1F-G**).

3.3. C5a signaling is required for melanoma and ICI-related microglial activation in the hippocampus

ICI treatment has been linked to several neurodegenerative consequences, including synaptic loss and microglial activation (8, 9, 21). Conversely, inhibiting C5a signaling has been found to counter proinflammatory consequences in the brain, including the polarization of inflammatory microglia in neurodegenerative conditions, including irradiated brain and AD (15, 17). We found elevated expression of microglial C5aR1 post-ICI treatment **(Fig. 1A-B)**. Thus, to evaluate the extent of neuroinflammatory damage post-ICI treatment and C5aR1-KO, we quantified microglial activation using the lysosomal (phagocytic) protein CD68 and IBA1 in the hippocampus. We conducted dual immunofluorescence confocal microscopy to assess the activated microglial landscape under melanoma, ICI treatment, and C5aR1-KO conditions (**Fig 2A-D**). First, vehicle-treated WT mice with or without melanoma displayed a comparable CD68-IBA-1 colocalization, whereas the melanoma-bearing C5aR1-KO mice (C5aR1-KO-MEL group) showed a significant decline and the lowest expression of CD68-IBA-1 immunoreactivity, compared to all groups (p*'s*<0.001). ICI-treated WT and C5aR1-KO mice without tumor showed the highest CD68-IBA-1 co-expression compared to vehicle-treated groups (**Fig. 2E-F**), demonstrating ICI-induced neuroinflammation in the brain. Notably, CD68-IBA1 expression was significantly declined in both groups in the presence of melanoma ($p<0.0001$ for WT-MEL-ICI and $p<0.01$ for C5aR1-KO-MEL-ICI, **Fig 2E**), signifying a change in inflammatory events post-cancer induction and ICI treatment. Three-way ANOVA found significant interactions of cancer × no cancer ($F_{(1, 61)} = 33.93$, $p<0.0001$), ICI × vehicle treatment ($F_{(1, 61)} = 4.041$, $p<0.05$), genotype × cancer ($F_{(1, 61)} = 6.449$, $p<0.002$), genotype × ICI treatment ($F_{(1, 61)} = 6.206$, $p<0.002$), and genotype × cancer × ICI treatment ($F_{(1, 61)} = 8.490$, $p<0.0003$). Taken together, these results indicate that C5aR1 antagonism after ICI treatment alleviates microglial activation.

3.4. Melanoma and ICI-related astrocytic hypertrophy is diminished in C5aR1-KO mice

Astrocytes maintain neurotransmitter and calcium balance in the brain and thereby support neuronal activity (22). Concurrent with microglial activation, we then assessed the impact of ICI treatment and C5aR1-KO on astrogliosis. We analyzed $GFAP^+$ astrocytic expression of the danger-associated molecular pattern (DAMP) marker toll-like receptor 4 (TLR4), a hallmark of astrocytic hypertrophy or astrogliosis commonly reported in brain injuries (15, 16). C5a-C5aR1

In review

signaling promotes neuroinflammation and astrogliosis and interacts with DAMP, including TLR4 signaling (23, 24). TLR4-GFAP colocalization was quantified across all experimental groups to assess the extent of astrogliosis following melanoma ICI therapy (**Fig 3A-D**). The C5aR1-KO-MEL group showed the lowest TLR4-GFAP immunoreactivity compared with the vehicle-treated and WT-MEL groups ($p<0.05$), indicating reduced astrocytic activity. In contrast, the WT-ICI group exhibited the highest level of astrogliosis (**Fig. 3C, F**), whereas the C5aR1-KO-ICI group showed a trend of reduced TLR4-GFAP expression. Importantly, both the WT-MEL-ICI and the C5aR1-KO-MEL-ICI mice had decreased TLR4-GFAP co-expression, with a greater reductions in the C5aR1-KO-MEL-ICI group, compared to their respective ICI-only treated (non-cancer) groups ($p<0.01$ and $p<0.001$, respectively, **Fig. 3E**). Three-way ANOVA indicated significant interactions of WT × KO genotype ($F_{(1, 39)} = 21.56$, $p<0.0001$), cancer × no cancer ($F_{(1, 39)} = 27.27$, $p<0.0001$), and genotype × cancer × ICI treatment ($F_{(1, 39)} = 4.704$, $p<0.04$). Overall, this result paralleled the microglial activation pattern and highlights the anti-gliosis role of C5aR1-KO following ICI treatment and cancer load.

In review

4 | DISCUSSION

The main goal of this study was to determine if ablation of complement anaphylatoxin C5a signaling via C5aR1 deletion confers protection against ICI-induced neuroinflammation. We found higher C5aR1 levels in microglia in human postmortem brains from ICI-treated patients. The comparison of ICI-treated cancer patients with non-tumor, non-ICI-exposed postmortem controls was dictated by tissue availability, quality, and anatomical comparability. Ideally, untreated melanoma patients or ICI-exposed non-cancer individuals would provide more informative comparisons; however, such cohorts are clinically scarce in postmortem repositories. Thus, we performed animal studies and found that, in the absence of tumor, ICI treatment alone elevated microglial C5aR1 expression in the brain. Prior studies have demonstrated that C5a-C5aR1 signaling promotes an immunosuppressive tumor microenvironment across multiple cancer types, including gastrointestinal and ovarian cancers, by recruiting myeloid-derived suppressor cells (MDSCs) and by excluding or modulating dysfunctional tumor-infiltrating immune cells (25-27). Consistent with this, our observation of reduced tumor growth in C5aR1-KO mice without ICI supports a role for C5aR1 signaling in shaping the solid tumor microenvironment. We acknowledge that peripheral immune cells expressing C5aR1, tumor-intrinsic effects on the immune microenvironment, and the developmental absence of C5aR1 during circuit maturation are plausible confounders that a global KO model cannot disentangle. We used this germline KO

as a proof of concept to test whether ablating global C5a/C5aR1 signaling modifies melanoma response and ICI-associated neuroinflammation. Critically, these findings provide a mechanistic scaffold for our primary translational objective: evaluating PMX205, a brain-penetrant C5aR1 inhibitor currently in Phase II trials for ALS, to mitigate ICI-induced CNS toxicity, as we have shown previously in the brain glioma radiation therapy model (15). Importantly, C5aR1 deficiency was not associated with diminished ICI-mediated tumor control under the conditions tested. Others have shown that pharmacological inhibition of C5aR1 can synergize with immune checkpoint blockade, particularly anti-PD-1 therapy, to enhance $CD8^+$ T cell-mediated cytotoxicity (26, 28). In our study, the lack of a pronounced difference in tumor burden between WT and C5aR1-KO mice under ICI treatment may reflect model-specific factors, including melanoma burden and the use of combination anti-PD-1 and anti-CTLA-4-based regimens versus anti-PD-1 monotherapy, which could influence the extent of the combined checkpoint inhibition.

Our prior work has demonstrated that combination ICI perturbs the CNS immune landscape, leading to upregulated microglial activation and T cell microglia interactions (8, 21). Our dual-immunofluorescence data support this finding, showing increased microglial activation and elevated astrogliosis in the WT mice treated with ICI alone. In contrast, C5aR1-KO mice exhibited significantly reduced astrocytic expression of the DAMP marker following ICI treatment, suggesting potential crosstalk between complement signaling and glial responses. These findings are supported by increased microglial C5aR1 expression in ICI-treated patient and rodent brains. Importantly, both microglial activation and astrogliosis were significantly attenuated in the ICI-treated melanoma group in C5aR1-KO mice compared to the WT-ICI-treated group, indicating an ICI-specific pro-inflammatory effect in the absence of tumor in the WT mice. Thus, opening new opportunities to counter ICI-induced neuroinflammation while preserving anti-tumor immunity. Finally, C5aR1-KO showed the most robust reduction in gliosis induced by melanoma burden alone, further underscoring its potential as a therapeutic mitigator by targeting C5aR1 signaling in cancer models. We found lower CD68-IBA1 and TLR4-GFAP co-localization in the WT melanoma + ICI groups than in the WT ICI-only groups. We propose two possibilities for this apparent reduction in neuroinflammatory markers. First, ICI-mediated tumor eradication in the melanoma + ICI group likely resolves the tumor-associated immune burden, thereby attenuating sustained microglial and astrocytic activation that would otherwise persist in the absence of effective tumor clearance. Second, tissue collection 8 weeks after ICI treatment ends represents a late post-treatment window, during which the acute neuroinflammatory response may have subsided. Supporting this interpretation, our recent spatial transcriptomics data (10) showed that microglia-mediated neurodegenerative events, including synaptic and myelin loss, occur as early

In review

as 72 hours post-ICI, and that increased proximity of activated microglia with neurons, astrocytes, and T cells drives early synaptic loss *in vivo*. The attenuated gliosis markers at later time points are therefore consistent with a model in which the peak neuroinflammatory response is an early, transient event.

Overall, our results demonstrate that C5aR1-KO exerts multifaceted effects, reducing melanoma growth while simultaneously modulating neuroinflammatory responses in the brain. This neuroprotective effect may mitigate cognitive impairment experienced by some melanoma patients following ICI treatment, thereby improving health outcomes and quality of life for cancer survivors. To enhance clinical relevance, future studies may incorporate pharmacological inhibition of C5aR1 with the brain-penetrant antagonist PMX205 to assess whether comparable therapeutic benefits are achieved in combination with ICI. Additionally, immune cell profiling by flow cytometry could elucidate changes in the systemic and CNS immune environments, providing deeper mechanistic insight into how targeting complement cascade signaling protects the brain from ICI-related neuroinflammation.

In review

ACKNOWLEDGEMENTS

We thank Prof. Robert Zeiser and Dr. Janki Manoja Vinnakota, Department of Hematology and Oncology, Freiburg University Medical Center, Germany, for kindly providing postmortem patient brain tissues. We thank Dr. Francesco Marangoni for providing the syngeneic murine melanoma cell line.

FUNDING

This work was supported by the National Institutes of Health (NIH) awards (R01CA251110, R01CA262213) to M.M.A., NIH NIAID R01AI121945 and R21AI144823 to S.O., Defense Health Agency award (ME250313) to S. O. and M. M. A. UCI CFCCC GRTH was supported by the NIH program project award P30CA062203.

DECLARATIONS

- Ethics approval: All animal experiments were approved by the UCI Institutional Animal Care and Use Committee (IACUC); all human tissue-related experiments were approved by the institutional ethics committees.
- Consent for publication: Not applicable
- Availability of data and materials: All data and materials are available upon request.
- Competing interests: The authors declare no competing interests

AUTHOR CONTRIBUTIONS

MMA conceptualized, designed, and supervised this study. KNN, AD, TNN, DS, and MGJ developed methodologies and acquired data. KNN, AD, DS, SO, & MMA carried out data analysis and interpretation. SO & MMA provided administrative, technical, or material support. KNN, AJT, SO, & MMA conducted writing, reviewing, and/or revising the manuscript.

In review

FIGURE LEGENDS

Fig. 1. (A) Elevated microglial C5aR1 expression in human postmortem brains from ICI-treated patients. Dual immunofluorescence staining and laser scanning confocal microscopy analysis (3-4 regions of interest per section, 3 sections per brain) for the microglial marker IBA1 and C5aR1 in the frontal cortex from patients receiving ICI treatment for different malignancies, compared with non-cancer, untreated control subjects. **(B)** Volumetric quantification of IBA1 and C5aR1 shows significantly increased immunoreactivity (****p<0.001) for microglial-C5aR1 co-labeling in the ICI-treated patients compared with non-cancer controls. **(C-D)** ICI treatment in WT, non-cancer mice significantly elevated (**p<0.02) microglial C5aR1 expression (IBA1-C5aR1) in the WT-ICI hippocampus compared to the vehicle-treated control group at two months post-ICI treatment. Data are presented as mean ± SEM (N = 3 subjects per group, **B**, and N = 5 mice per group, **D**). P values were derived from an unpaired two-tailed *t* tests. Scale bars, 20 μm (**A**), 7 μm (**C**, Control), and 5 μm (**C**, WT-ICI).

In review

(E) Experimental Timeline. 3-month-old C5aR1 knockout (C5aR1-KO) and wild-type (WT, C57BL/6) mice received either melanoma cells (D4M.3A-UV2, 5×10^5 cells per site, bilateral intradermal injections,) or phosphate-buffered saline (PBS). Seven days post-cancer induction, the respective mouse groups were treated with either combination ICI, including anti-CTLA4 (twice weekly, IP, 1000 μg) and anti-PD-1 (thrice weekly, IP, 200 μg), or vehicle for three weeks. In parallel with the ICI treatment, tumors were measured using a caliper twice a week for a month, followed by euthanasia and tissue collection.

(F-G) Tumor Growth. Each plot shows individual tumor sizes for each experimental group **(F)** and the group average **(E)**. ICI treatment in WT or C5aR1 KO mice significantly reduced tumor growth compared to the vehicle-treated group, indicating its therapeutic efficacy. Tumor growth was dampened in the C5aR1-KO background without ICI treatment (purple). Data are presented as mean ± SEM (N = 8-10 mice/group). P values were derived from two-way ANOVA and Bonferroni's multiple comparisons test. $^{+}$p<0.05, $^{++++}$p<0.001 for WT-MEL vs. WT-MEL-ICI and C5aR1-MEL-ICI comparisons. *p<0.05, ****p<0.001 WT-MEL vs. C5aR1-KO-MEL comparisons.

Figure 2. Impact of C5aR1-KO and ICI treatment on neuroinflammation.

(A–D) Representative confocal photomicrographs of CD68-IBA1 colocalization (magenta and green, respectively, **A, C**) and CD68 single-channel (magenta, **B, D**) in the hippocampal dentate gyrus (blue, DAPI nuclear staining).

(E) Quantitative volumetric analysis of microglial activation (colocalization of lysosomal protein CD68 and a pan-microglial marker IBA-1).

(F) A representative 3D surface rendering of $CD68^+$ immunoreactive puncta (magenta) colocalized with the $IBA\text{-}1^+$ microglial cell surface (green) from the WT-ICI group (arrow, **C**).

Data are presented as mean ± SEM (N = 4-8 mice/group). P values were derived from three-way ANOVA and Bonferroni's multiple comparisons test. *p ≤ 0.05. **p ≤ 0.01. ***p ≤ 0.001. ****p ≤ 0.0001. Scale bars: 100 μm (**A-D**), 10 μm (**F**).

Figure 3. Impact of C5aR1 KO and ICI treatment on astrogliosis.

(A–D) Representative confocal photomicrographs of GFAP-TLR4 colocalization (green and red, respectively, **A, C**) and TLR4 single-channel (red, **B, D**) in the hippocampal dentate hilus (blue, DAPI nuclear staining).

(E) Quantitative volumetric analysis of the astrocytic expression of the danger-associated molecular pattern (DAMP) marker, toll-like receptor 4 (TLR4).

(F) A representative 3D surface rendering of $TRL4^+$ immunoreactive puncta (red) colocalized with the $GFAP^+$ astrocyte (green) from the WT-ICI group (arrow, **C**).

Data are presented as mean ± SEM (N = 4-8 mice/group). P values were derived from three-way ANOVA and Bonferroni's multiple comparisons test. *p ≤ 0.05. **p ≤ 0.01. ****p ≤ 0.0001. Scale bars: 30 μm (**A-D**), 10 μm (**F**).

In review

REFERENCES

1. Buder-Bakhaya K, Hassel JC. Biomarkers for Clinical Benefit of Immune Checkpoint Inhibitor Treatment-A Review From the Melanoma Perspective and Beyond. Front Immunol. 2018;9:1474.
2. Mc Neil V, Lee SW. Advancing Cancer Treatment: A Review of Immune Checkpoint Inhibitors and Combination Strategies. Cancers (Basel). 2025;17(9).
3. Miller SR, Schipper M, Fritsche LG, Jiang R, Strohbehn G, Otles E, et al. Pan-Cancer Survival Impact of Immune Checkpoint Inhibitors in a National Healthcare System. Cancer Med. 2024;13(21):e70379.
4. Hargadon KM, Johnson CE, Williams CJ. Immune checkpoint blockade therapy for cancer: An overview of FDA-approved immune checkpoint inhibitors. Int Immunopharmacol. 2018;62:29–39.
5. Darnell EP, Mooradian MJ, Baruch EN, Yilmaz M, Reynolds KL. Immune-Related Adverse Events (irAEs): Diagnosis, Management, and Clinical Pearls. Curr Oncol Rep. 2020;22(4):39.
6. Das S, Johnson DB. Immune-related adverse events and anti-tumor efficacy of immune checkpoint inhibitors. J Immunother Cancer. 2019;7(1):306.
7. Sayer M, Agrawal P, Ng DQ, Kagramanov D, Trudeau J, Othy S, et al. Incidence and predictors of immune checkpoint inhibitor treatment-related cognitive impairment in a racial and ethnic diverse population. Supportive care in cancer : official journal of the Multinational Association of Supportive Care in Cancer. 2025;33(6):523.
8. Ifejeokwu OV, Do AH, El Khatib SM, Ho NN, Zavala A, Othy S, et al. Immune checkpoint inhibition perturbs neuro-immune homeostasis and impairs cognitive function. J Exp Clin Cancer Res. 2025;44(1):183.
9. Vinnakota JM, Adams RC, Athanassopoulos D, Schmidt D, Biavasco F, Zahringer A, et al. Anti-PD-1 cancer immunotherapy induces central nervous system immune-related adverse events by microglia activation. Sci Transl Med. 2024;16(751):eadj9672.
10. Swami D, El-Khatib SM, Sureshchandra S, Nguyen E, Vinnakota JM, Zeiser R, et al. Spatial Transcriptomics Reveals a T Cell-Mediated Microglial Activation Axis of Immune Checkpoint Inhibition-Related Adverse Events in the Brain. Adv Sci (Weinh). 2026:e77733.
11. Goldberg SB, Gettinger SN, Mahajan A, Chiang AC, Herbst RS, Sznol M, et al. Pembrolizumab for patients with melanoma or non-small-cell lung cancer and untreated brain metastases: early analysis of a non-randomised, open-label, phase 2 trial. The Lancet Oncology. 2016;17(7):976–83.
12. Rogiers A, Leys C, Lauwyck J, Schembri A, Awada G, Schwarze JK, et al. Neurocognitive Function, Psychosocial Outcome, and Health-Related Quality of Life of the First-Generation Metastatic Melanoma Survivors Treated with Ipilimumab. J Immunol Res. 2020;2020:2192480.
13. Luijendijk MJ, Albers EAC, Egeler M, van de Poll-Franse LV, Blank CU, Schagen SB. Long-term cognitive function after treatment with immune checkpoint inhibition for melanoma. Journal of cancer survivorship : research and practice. 2026.
14. Gomez-Arboledas A, Acharya MM, Tenner AJ. The Role of Complement in Synaptic Pruning and Neurodegeneration. Immunotargets Ther. 2021;10:373–86.
15. Krattli RP, Do AH, El-Khatib SM, Alikhani L, Markarian M, Vagadia AR, et al. C5aR1 inhibition alleviates cranial radiation-induced cognitive decline. Cancer Res. 2025.
16. Markarian M, Krattli RP, Jr., Baddour JD, Alikhani L, Giedzinski E, Usmani MT, et al. Glia-Selective Deletion of Complement C1q Prevents Radiation-Induced Cognitive Deficits and Neuroinflammation. Cancer Res. 2021;81(7):1732–44.
17. Schartz ND, Liang HY, Carvalho K, Chu S-H, Mendoza-Arvilla A, Petrisko TJ, et al. C5aR1 antagonism suppresses inflammatory glial responses and alters cellular signaling in an Alzheimer's disease mouse model. Nature communications. 2024;15(1):7028.
18. Muller-Jensen L, Mohn N, Skripuletz T, Carl S, Thomas J, Grote-Levi L, et al. Complement activation profiles in patients with immune checkpoint inhibitor-associated neuromuscular immune-related adverse events. Journal of neurology. 2025;272(7):459.

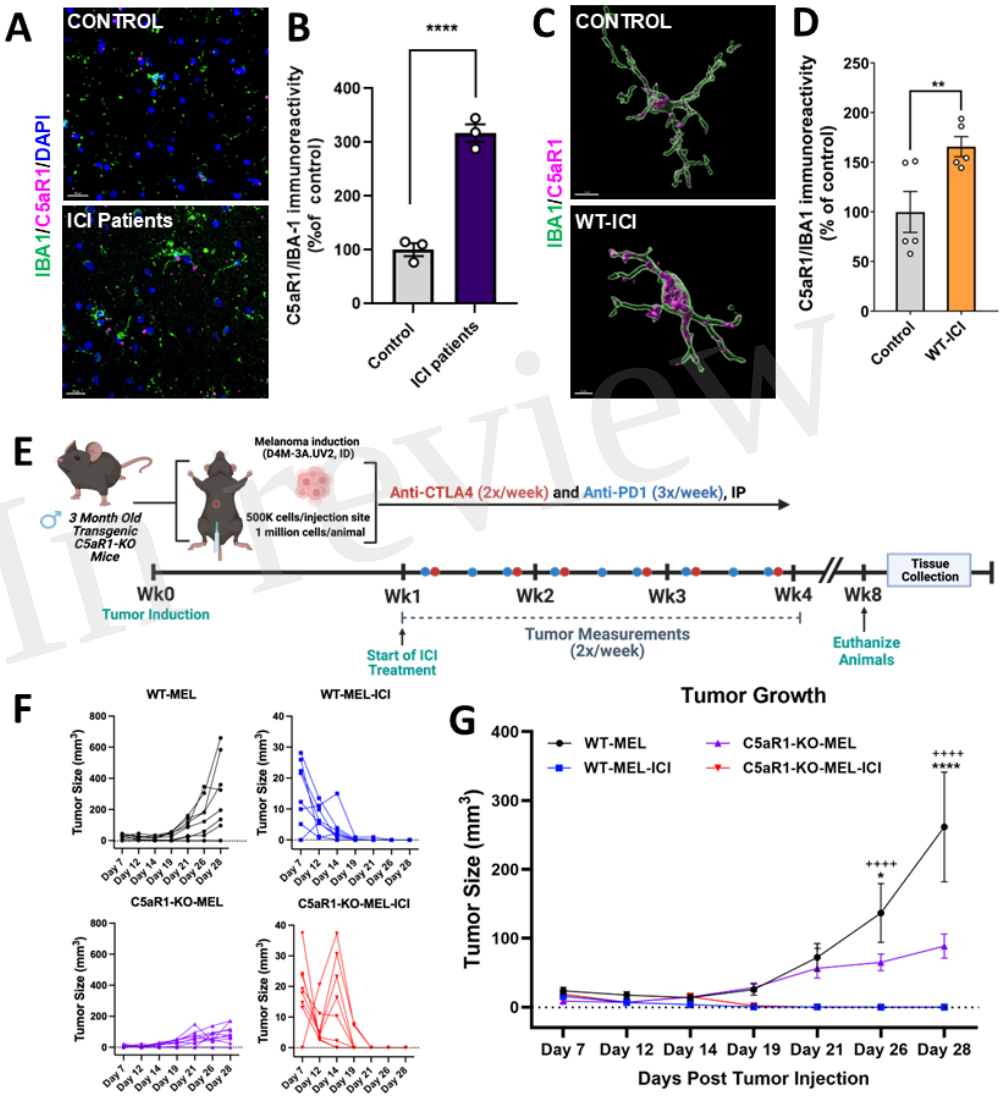
In review

19. Muller-Jensen L, Schulz AR, Mei HE, Mohr R, Ulrich C, Knape P, et al. Immune signatures of checkpoint inhibitor-induced autoimmunity-A focus on neurotoxicity. Neuro-oncology. 2024;26(2):279–94.
20. Hollmann TJ, Mueller-Ortiz SL, Braun MC, Wetsel RA. Disruption of the C5a receptor gene increases resistance to acute Gram-negative bacteremia and endotoxic shock: opposing roles of C3a and C5a. Mol Immunol. 2008;45(7):1907–15.
21. Swami D, Sureshchandra S, Vinnakota JM, Zeiser R, Othy S, Acharya MM. Spatial Transcriptomics reveals a T cell-mediated microglial activation axis of neurodegeneration following immune checkpoint inhibition. bioRxiv. 2026.
22. Araque A, Carmignoto G, Haydon PG, Oliet SH, Robitaille R, Volterra A. Gliotransmitters travel in time and space. Neuron. 2014;81(4):728–39.
23. Tenner AJ. Complement-Mediated Events in Alzheimer's Disease: Mechanisms and Potential Therapeutic Targets. Journal of immunology. 2020;204(2):306–15.
24. Zhang X, Kimura Y, Fang C, Zhou L, Sfyroera G, Lambris JD, et al. Regulation of Toll-like receptor-mediated inflammatory response by complement in vivo. Blood. 2007;110(1):228–36.
25. Shen H, Gu X, Li X, Xiang Z, Zhang R, Shi F, et al. C5aR1 shapes a non-inflammatory tumor microenvironment and mediates immune evasion in gastric cancer. Biomol Biomed. 2023;23(3):392–404.
26. Zhang C, Cao K, Yang M, Wang Y, He M, Lu J, et al. C5aR1 blockade reshapes immunosuppressive tumor microenvironment and synergizes with immune checkpoint blockade therapy in high-grade serous ovarian cancer. Oncoimmunology. 2023;12(1):2261242.
27. Beach C, MacLean D, Majorova D, Melemenidis S, Nambiar DK, Kim RK, et al. Improving radiotherapy in immunosuppressive microenvironments by targeting complement receptor C5aR1. J Clin Invest. 2023;133(23).
28. Ajona D, Ortiz-Espinosa S, Moreno H, Lozano T, Pajares MJ, Agorreta J, et al. A Combined PD-1/C5a Blockade Synergistically Protects against Lung Cancer Growth and Metastasis. Cancer Discov. 2017;7(7):694–703.

In review

Figure 1.TIF

Revised Figure 1.



In review

Figure 2.TIF

Revised Figure 2.

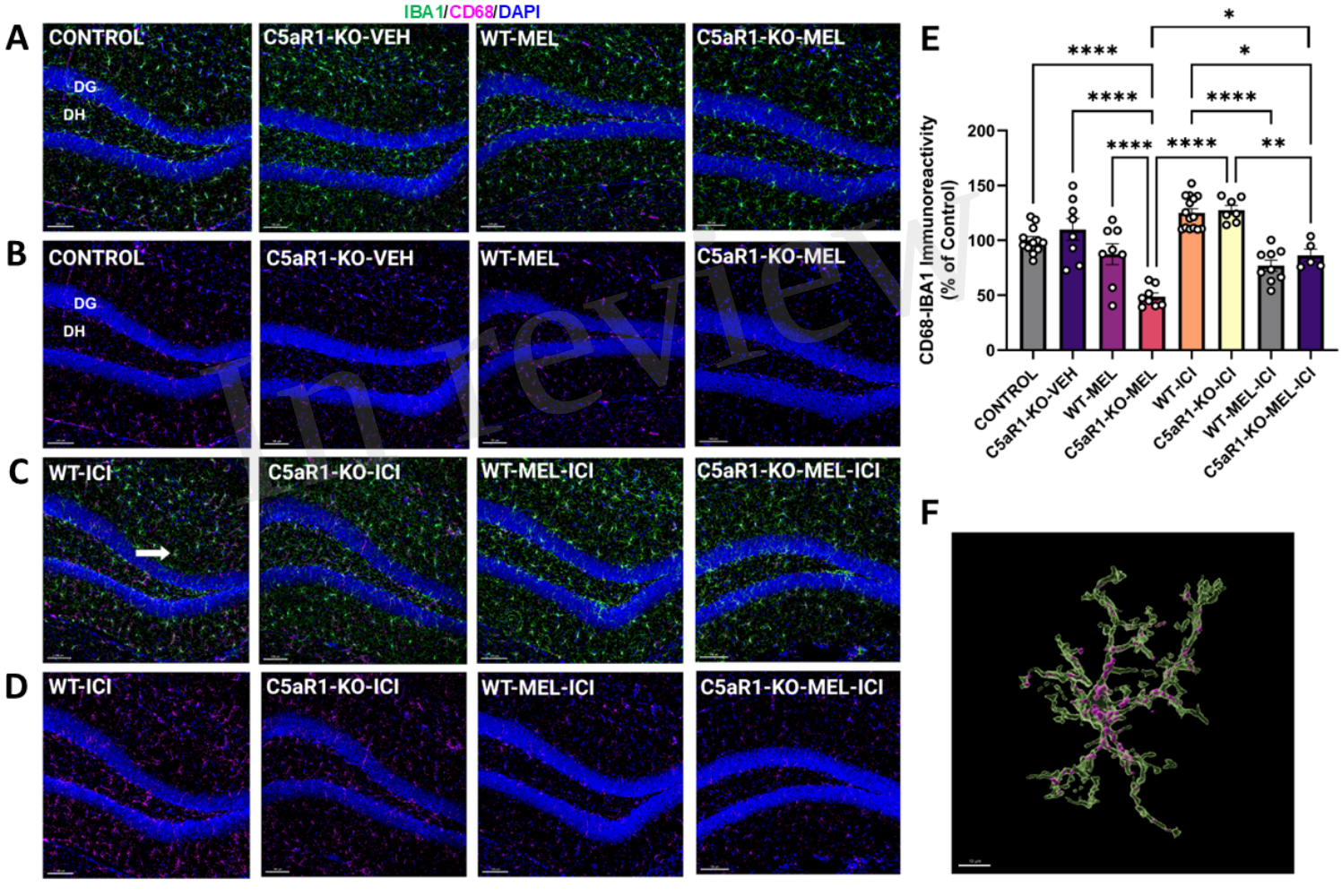


Figure 3.TIF

Revised Figure 3.

